Journal of Hazardous Materials 394 (2020) 122486

Contents lists available at ScienceDirect

Journal of Hazardous Materials

journal homepage: www.elsevier.com/locate/jhazmat

High temperature silicon-carbide-based flexible electronics for monitoring hazardous environments

Hoang-Phuong Phan[a,*], Toan Dinh[a,c], Tuan-Khoa Nguyen[a], Afzaal Qamar[d], Thanh Nguyen[a], Van Thanh Dau[a,b], Jisheng Han[a], Dzung Viet Dao[a,b], Nam-Trung Nguyen[a]

[a] *Queensland Micro and Nanotechnology Centre, Griffith University, Queensland, Australia*
[b] *School of Engineering and Built Environment, Griffith University, Queensland, Australia*
[c] *School of Engineering, University of Southern Queensland, Queensland, Australia*
[d] *Electrical Engineering and Computer Science, University of Michigan, MI, USA*

GRAPHICAL ABSTRACT

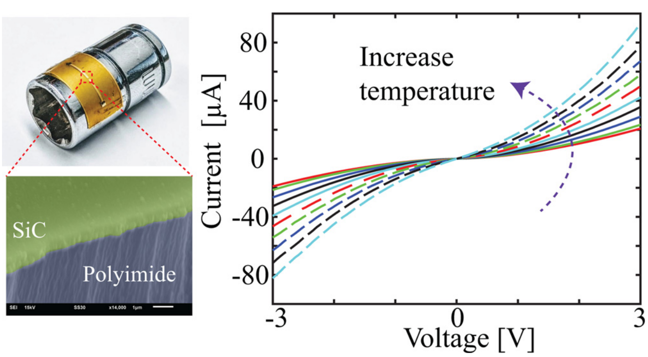

ARTICLE INFO

Editor: Dr. Rinklebe Jörg

Keywords:
Silicon carbide
Flexible electronics
Environment monitoring
Hazardous environments

ABSTRACT

With its unprecedented properties over conventional rigid platforms, flexible electronics have been a significant research topic in the last decade, offering a broad range of applications from bendable display, flexible solar-energy systems, to soft implantable-devices for health monitoring. Flexible electronics for harsh and hazardous environments have also been extensively investigated. In particular, devices with stretchability and bend-ability as well as tolerance to extreme and toxic operating conditions are imperative. This work presents silicon carbide grown on silicon and then transferred onto polyimide substrate as a new platform for flexible sensors for hostile environments. Combining the excellent electrical properties of SiC and high temperature tolerance of polyimide, we demonstrated for the first time a flexible SiC sensors that can work above 400 °C. This new sensing platform opens exciting opportunities toward flexible sensing applications in hazardous environments.

1. Introduction

Recent advancements in soft-lithography and printing technologies have made tremendous progress in the development of stretchable and bendable electronics, providing new exciting functionality over conventional hard, rigid platforms (Jeong et al., 2018; Rogers et al., 2010; Nathan et al., 2012; Phan et al., 2019a; Falahi et al., 2019). A broad range of flexible applications have been translated from basic-research

* Corresponding author.
E-mail address: h.phan@griffith.edu.au (H.-P. Phan).

https://doi.org/10.1016/j.jhazmat.2020.122486
Received 1 December 2019; Received in revised form 31 January 2020; Accepted 5 March 2020
Available online 20 March 2020
0304-3894/

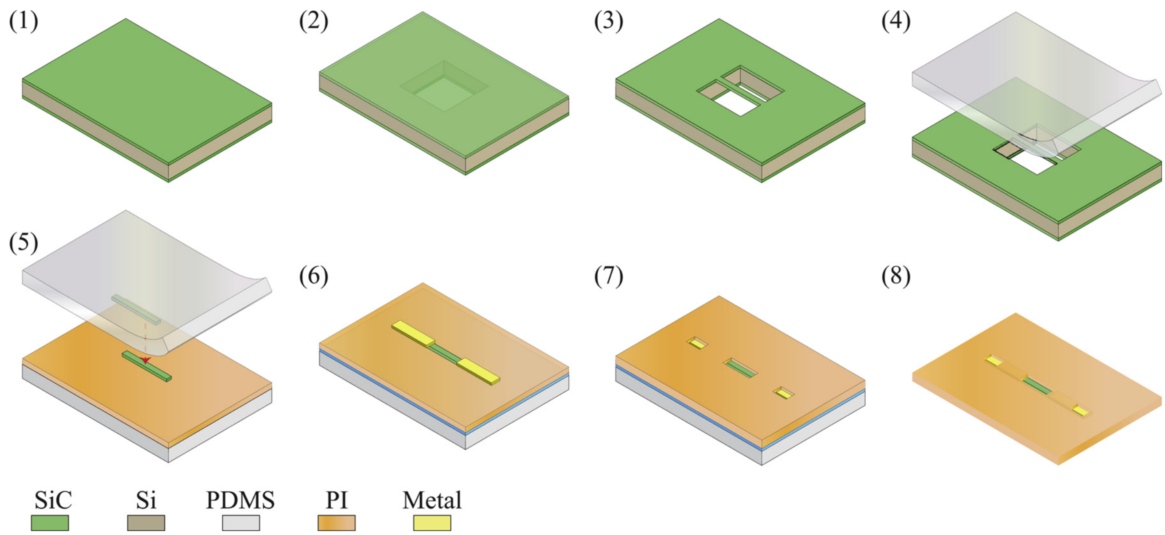

Fig. 1. Schematic sketch of the fabrication process. (1) SiC/Si platform; (2) free-standing SiC membranes; (3) suspended SiC micro-bridges; (4) picking using PDMS; (5) transfer onto PI/glass; (6) metallization; (7) encapsulating with another PI layer; (8) peeling-off.

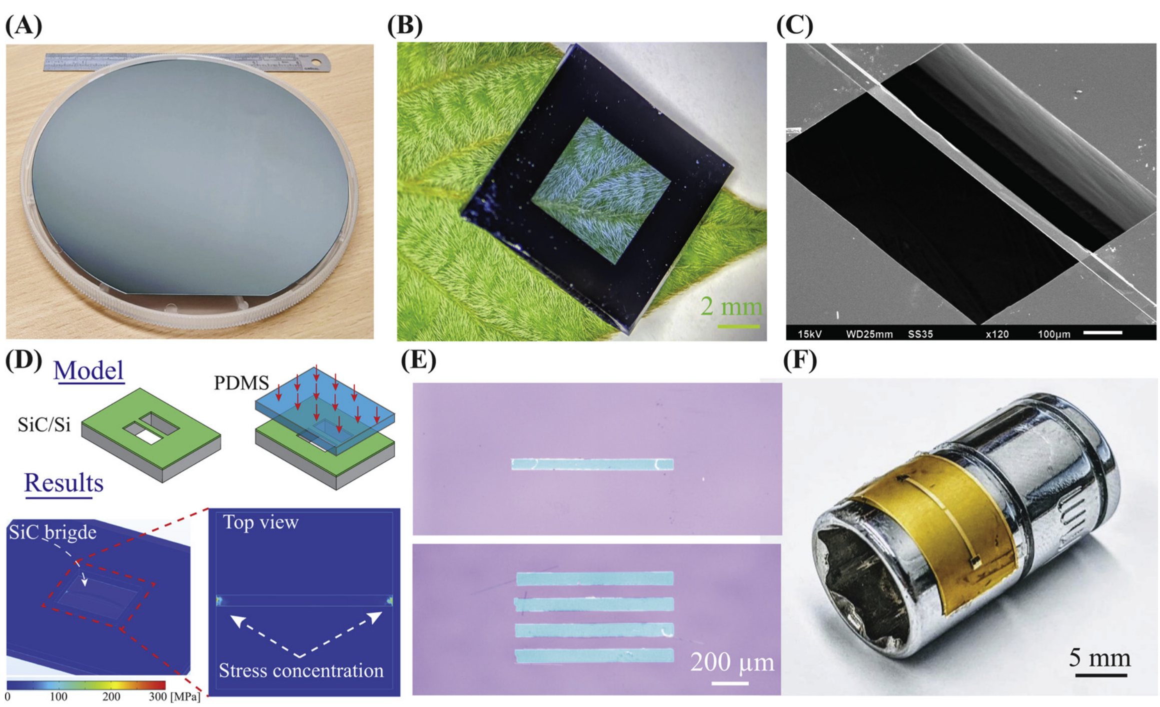

Fig. 2. Photograph and SEM images of fabricated devices. (A) Photograph of a full SiC-on-Si wafer; (B) photogrpah of released transparent-SiC membrane; (C) SEM image of a free standing SiC microbride released from the Si substrate; (D) finite element analysis of the stress concentration on the SiC microbridges under PDMS stamping; (E) microscopy images of SiC bridges attached on the PDMS stamp (top: 875 µm × 50 µm single-bridge; bottom: 875 µm × 100 µm bridge-array); (F) demonstration of the flexibility of the SiC-on-PI platform.

into commercial products, including bendable displays, smart-watches for biometric-data tracking, and wearable ultraviolet dosimeters. Although organic materials and conductive polymers offer the intrinsic bendable property, most of the commercialized devices are built based on conventional inorganic semiconductors which are transferred from the rigid substrates onto a soft and flexible template (Sun and Rogers, 2007; Liu et al., 2015). The use of common inorganic semiconductors such as silicon and III-nitride takes advantage of their advanced fabrication technologies as well as the established physics (Yu et al., 2017; Zhang et al., 2019).

Typical flexible applications operate at a small temperature range varying from room temperature to approximately 150 °C (Jeon et al., 2013; Dinh et al., 2019, 2017; Zhan et al., 2014). Recent studies suggests an increasing demand for devices that can operate at a wider range of temperatures varying from cryogenic up to several hundred degree Celsius (Almuslem et al., 2019; Sun et al., 2018; Chen et al., 2016; Li et al., 2015). This is quite obvious in space exploration industry, where the temperature can be reduced to below −250 °C for the case of Jupiter or can reach to above 400 °C on Venus surface (Phan et al., 2018; Hunter et al., 2006; So and Senesky, 2017). NASA has been taking part in developing a host of deployable structures including balloons, solar sails, space-borne telescopes and membrane-based synthetic aperture radars to work at these temperatures (Brandon et al., 2004, 2011; Basirico et al., 2017). To develop each of these applications, a thin, low mass, large area structure (i.e., polymer-based) is an imperative component. Additionally, integration of sensors within these

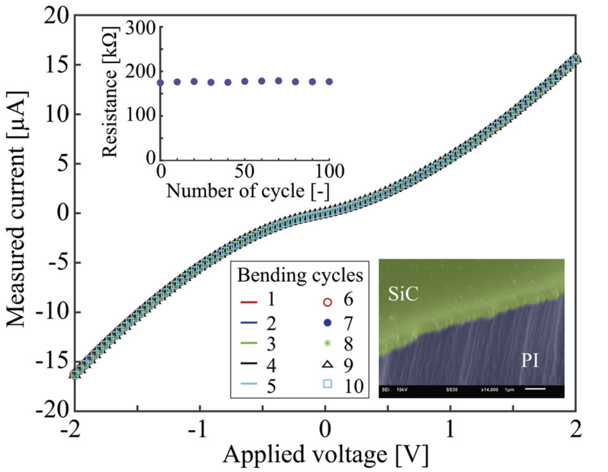

Fig. 3. Mechanical stability of the SiC-on-PI devices subjected to the bending experiment. Inset: Demonstration of SiC-on-PI device being wrapped around a curved surface with a radius of 5 mm (top); and SEM image of SiC/PI interface after bending (bottom).

structures is of significant importance. Furthermore, considering the fact that every milligram launched to space does matter for the associated cost, having electronics devices on a light-weight, flexible platform could ease the installation and significantly reduce the launching expense (Meador, 2019). Aside from high temperatures, chemical/mechanical corrosion and high radiation are other hazardous factors that can adversely affect the performance of flexible electronics. Well-known examples for these extreme conditions are deep sea exploration and underwater environmental monitoring systems, where salty water could rapidly degrade device performance (Nassar et al., 2018; Shaikh et al., 2019). As a consequence, there is a need for developing niche electronics that can withstand these extreme environments.

Main-stream flexible inorganic devices have been developed based on silicon (Si) nanothin films. Nevertheless, due to its relatively fast hydrolysis rate, Si electronics gradually degrade when being subjected to a long-term underwater operation (Yin et al., 2015; Hwang et al., 2015). Furthermore, at high temperature the thermally activated intrinsic carriers make the performance of Si-based devices no longer reliable (Li et al., 2018). Silicon carbide (SiC) has emerged as an excellent alternative owing to its robust physical properties (Phan et al., 2019b; Mandrusiak et al., 2018; Yang et al., 2019b; Nguyen et al., 2017). Silicon carbide-based transistors, pressure sensors, photodetectors operating in extreme environments have been successfully demonstrated (Lanni et al., 2013; Nguyen et al., 2018; Yang et al., 2019a). However, as these devices were built either in the bulk-form or from a SiC epilayer on a solid substrate (Qamar et al., 2015), SiC-based electronics with mechanical flexibility that can operate at high temperatures have been rarely reported.

We present here ultra-thin silicon carbide (SiC) nanomembranes on a soft, thin polyimide substrate as a robust platform for flexible electronics working in harsh environments, taking advantage of the electrical stability and chemical inertness of the SiC material. The low mechanical bending stiffness of SiC nanomembranes combined with the intrinsic softness of micro-thick polyimide enable excellent flexibility. As a proof of concept, we demonstrate an Al-doped SiC film on polyimide as a temperature sensors that can work above 400 °C, the highest working temperature reported so far on flexible electronics based on wide-band-gap materials.

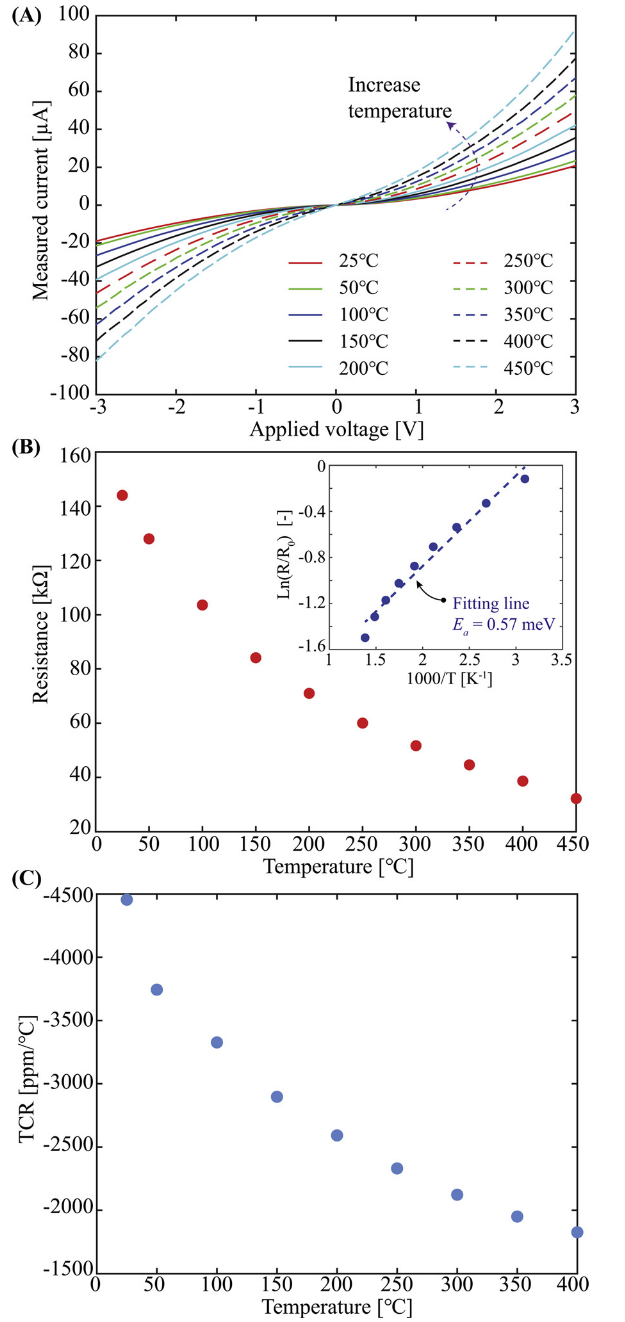

Fig. 4. SiC-on-PI for temperature sensors (a) *I–V* curve under temperature variation; (b) resistance change vs. temperatures. Inset: Relationship between ln (R/R_0) and 1000/*K* in Kelvin to fit the parameters in Eq. (3); (c) TCR vs. temperatures.

2. Experimental procedures

2.1. Preparation of SiC films

We deposited the 3C-SiC films on both sides of a 6-in. (100)-silicon wafer using a hot wall chemical vapor deposition chamber at 1250 °C. Prior to the growth process the silicon wafer was cleaned using the RCA standard. The deposition process started with a carbonization step to form a growth-buffer layers. Silane and propane were then alternatively supplied to stack SiC layers onto the buffer layer. Trimethyaluminum (TMAl) was employed to form a normally doped p-type 3C-SiC with a carrier concentration of approximately 10^{18} cm^{-3}. The thickness of SiC film was measured as 130 nm using Nanometrics Nanospec™ AFT210.

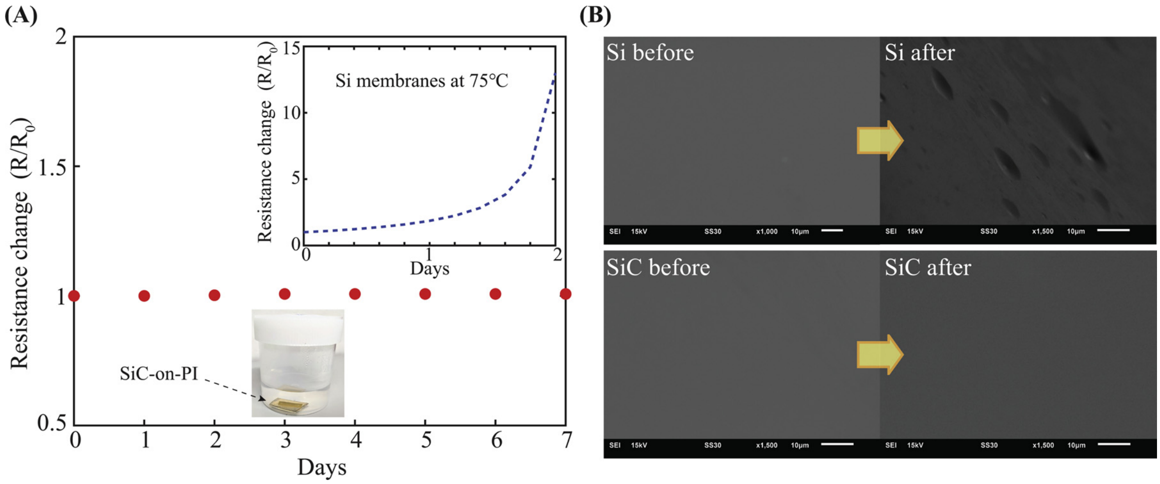

Fig. 5. Testing of SiC-on-PI under high humidity and corrosive condition. (A) The electrical conductivity of SiC in comparison to Si nanomembranes soaken in PBS at 75 °C. Inset: Estimated resistance change in 130 nm-thick Si membranes based on the hydrolysis rate; (B) surfaces of SiC and Si subjected to ammonium salt (TMAH).

The detail of the growth process can be found in our previous studies, where the crystallinity and orientation of the SiC films have been reported (Wang et al., 2011; Nguyen et al., 2019).

2.2. Transferring SiC onto flexible substrate

Fig. 1 illustrates the fabrication process of the flexible SiC devices, which is compatible with the standard photolithography technology. Following the deposition process, SiC micro windows on the backside was patterned using inductive plasma etching (ICP), exposing the Si substrate. The exposed Si areas were then removed using KOH etching at 80 °C, leaving free-standing SiC membranes with a dimension of 875 µm × 875 µm. Due to its chemical inertness, the SiC thin film on the back functioned as the hard-mask for Si wet etching. Next, lithography was applied to the released SiC membranes, followed by ICP etching to define free-standing SiC micro-bridge structures. These micro bridges were then picked up using a PDMS (1:10 ratio) stamp. By utilizing a stress concentration phenomenon, SiC bridges were detached from the Si layer at the supporting anchors. Next, the stamped SiC micro-structures were transferred onto a polyimide (PI) film that was pre-spincoated on a glass substrate. Due to the higher adhesion force between the uncured PI and SiC compared to SiC/PDMS, the SiC films remained on the PI substrate upon removing the PDMS stamp. Subsequently, metal (Au/Cr – 100 nm/10 nm) was ebeam evaporated and patterned to form electrodes for the SiC devices. The samples were then annealed at 400 °C to cure the PI as well as to enhance the contact between metal and semiconductor. Finally, the SiC-on-PI devices were peeled off from the glass substrate, leaving a SiC-based flexible electronic platform.

2.3. Bending experiments

After being removed from the handling substrate, the sample was mounted onto a linear actuator to induce mechanical load onto the flexible device. A bending radius of $R = 5$ mm was applied to the samples with 100 cycles. The induced strain was approximated as $\varepsilon = [t/2]/R$, where t is the thickness of the polyimide film. Electrical measurement was performed before and after the bending cycles to evaluate the stability of the device subjected to mechanical stimulation.

2.4. Electrical characterization at high temperatures

The current–voltage characteristics (*I–V*) of the SiC on PI temperature sensors were characterized using a semiconductor device parameter analyzer Agilent™ A1500, by sweeping applied voltages from −3 V to 3 V. The samples was mounted onto a temperature-controlled thermal chuck (Linkam Probe stage HSF600E). The *I–V* curve of the SiC devices was then recorded at different chuck temperatures with an increment of approximately 50 K. The surface temperature was monitored using a K-type thermocouple.

3. Results and discussion

Fig. 2 shows photographs of the fabricated devices. The large scale of the SiC-Si platform (Fig. 2(a)) along with the compatibility with standard micromachining processes could enable wafer-scale level fabrication of flexible SiC electronics. The transparency of released SiC nanomembranes (Fig. 2(b)) allow for the alignment of subsequent photography masks with the pre-defined free-standing structures. The simulation results (Comsol Multiphysics™) shown in Fig. 2(d) indicates that under pressurizing the PDMS stamp onto the free-standing SiC micro-bridges, stress was concentrated at the supporting edges. The finite element method (FEM) was consistent with the experimental results, where the SiC bridges was separated from the Si substrate at the anchor parts, and firmly attached on the PDMS stamp, Fig. 2(E). Upon removing from the handling glass layer, the SiC-on-PI sensors show excellent flexibility, as demonstrated in Fig. 2(F).

Fig. 3 shows the *I–V* characteristics of a SiC device. The non-linear behavior of the current–voltage curve suggests a Schottky contact due to the barrier height between Au and p-type 3C-SiC (Kojima et al., 2000). The devices were then subjected to the bending test using the aforementioned linear actuators. No delamination was observed after bending the device, demonstrating the strong bonding between SiC and the PI substrate. The consistency of the electrical conductance after 100 bending cycles further confirmed the excellent stability of the SiC-on-PI subjected to mechanical deformation. The inset figure shows an SEM image of the SiC/PI interface, indicating that the sample was free of delamination and crack. It should be pointed out that the bending stiffness (M) of a solid beam with Young's modulus E and a thickness t is $M = Et^3/12$. The use of nanothin SiC films on a soft and thin PI substrate significantly reduces the bending stiffness, thereby enabling large mechanical deformation. Our experimental results demonstrated that transferring SiC membranes on to a soft substrate enables new flexible functionality where the conventional bulk-SiC-based platform cannot offer. The electrical conductance of the p-type SiC was then investigated under the variation of temperature from 25 °C up to 450 °C. Experimental results showed that increasing temperature resulted in increasing the current in the SiC sensors, Fig. 4(A). The *I–V* curve also returned to its initial value when cooling down to room temperature. The change in the electrical conductivity of the SiC films is attributed to the increase of charge carriers due to thermal activation as well as the decrease in the hole mobility due to the enhanced phonon-hole scattering (Dinh et al., 2016). The temperature dependence of hole concentration (N_{SiC}) in p-type SiC sensors can be approximated as:

$$N_{\mathrm{SiC}} \sim T^{3/2}\exp(E_a/k_B T) \quad (1)$$

where E_a is thermal activation energy of the Al dopants and k_B is Boltzmann constant. On the other hand, the decrease in the hole mobility (μ_{SiC}) at elevated temperatures can be simply determined as:

$$\mu_{\mathrm{SiC}} \sim T^{-\alpha} \quad (2)$$

where α is an experimental constant. As a consequence, the electrical conductivity can be determined as follows:

$$\sigma_{\mathrm{SiC}} = q\mu N_{\mathrm{SiC}} \sim T^{3/2-\alpha}\exp(E_a/k_B T) \quad (3)$$

Based on this model, the activation energy of the p-type SiC films was estimated to be 57 meV, Fig. 4(B), inset. The temperature coefficient of resistance of the SiC films ($TCR = (\Delta R/R)/\Delta T$) was found to be 4500 ppm/°C at room temperature and decreased to 1800 ppm/°C at 400 °C, Fig. 4(C). The large TCR in a wide range of temperatures suggests that SiC-on-PI platform is an excellent candidate for thermal sensing applications. The decrease in the TCR at elevated temperatures could be attributed to the saturation of the ionized impurity along with a more dominant role of the diminution of the hole mobility (Dinh et al., 2016).

Besides high temperatures, the capability of flexible devices in fluidics and corrosive environments is also of significant interest. We characterized the electrical properties of the SiC-on-PI in fluidics by soaking the sample in Phosphate-Buffered Saline (PBS) pH 7.4 at 75 °C for an accelerated test. The resistance of the SiC films remained unchanged after 7 days, Fig. 5(A). As a means to compare, we estimated the change in the resistance of 130 nm-thick Si nanomembranes under the same condition using the hydrolysis rate reported by Lee et al. (2017). Accordingly, Si membranes with a carrier concentration of $10^{18}\,\mathrm{cm}^{-3}$ experience a dissolving rate of over 60 nm/day. This corresponds to an increase in resistance of 1200% after 2 days in PBS at 75 °C, Fig. 5(A) Inset. Furthermore, the corrosive test was performed by soaking SiC and Si samples into ammonium salt (TMAH) at 80 °C for 10 h. While the surface of Si was significantly attacked, no-observable surface morphology change was detected in the SiC sample, Fig. 5(B). These results emphasize the advantage of the SiC-on-PI platform for applications used in underwater and highly corrosive environments.

4. Conclusion

This work reports on the development and characterization of flexible crystalline silicon carbide sensors operating at elevated temperatures up to 450 °C. The experimental results showed the high feasibility of transferring silicon carbide nanothin films from the hosting Si substrate onto a soft platform, enabling the integration of SiC-based flexible electronics. The experimental data indicated a good bonding adhesion between SiC and polyimide, with excellent mechanical flexibility and stability. The new sensing platform exhibited a good thermal sensitivity, with a broad working temperature range varying from 25 °C to 450 °C. Combining with the chemical inertness of SiC, the developed devices show great potential for sensing applications in harsh and hazardous environments, with new capability of bendable and wrappable around curved surfaces.

Authors' contribution

H.-P.P., T.D. fabricated the devices. H.-P.P. and T.N. conducted the thermosensitive measurement. T.-K.N., A.Q. did the FEM simulation. H.P.P. and J.H. took the SEM images. All authors analyzed the experimental results. H.-P.P. and N.-T.N. designed and supervised the project. The manuscript was written through contributions of all authors. All authors have given approval to the final version of the manuscript.

Conflict of interest

None declared.

Acknowledgments

This work was partially funded by the research grants LP160101553 andDE200100238 from the Australian Research Council (ARC). The 3C-SiC material was developed and supplied by Leonie Hold and Alan Iacopi of the Queensland Microtechnology Facility, part of the Queensland node, Griffith of the Australian National Fabrication Facility, a company established under the National collaborative Research Infrastructure Strategy to provide nano and microfabrication facilities for Australia's researchers. H.P.P. acknowledges research grants from Griffith University Research Infrastructure Program.

References

Almuslem, A.S., Shaikh, S.F., Hussain, M.M., 2019. Flexible and stretchable electronics for harsh-environmental applications. Adv. Mater. Technol. 4, 1900145.
Basirico, L., Basile, A.F., Cosseddu, P., Gerardin, S., Cramer, T., Bagatin, M., Ciavatti, A., Paccagnella, A., Bonfiglio, A., Fraboni, B., 2017. Space environment effects on flexible, low-voltage organic thin-film transistors. ACS Appl. Mater. Interfaces 9, 35150–35158.
Brandon, E., West, W., Zhou, L., Jackson, T., Theriot, G., Devine, R.A., Binkley, D., Verma, N., Crawford, R., 2004. Flexible electronics for space applications. MRS Online Proc. 814.
Brandon, E.J., Vozoff, M., Kolawa, E.A., Studor, G.F., Lyons, F., Keller, M.W., Beiermann, B., White, S.R., Sottos, N.R., Curry, M.A., Banks, D.L., 2011. Structural health management technologies for inflatable/deployable structures: integrating sensing and self-healing. Acta Astronaut. 68, 883–903.
Chen, S., Shang, M., Gao, F., Wang, L., Ying, P., Yang, W., Fang, X., 2016. Extremely stable current emission of p-doped SiC flexible field emitters. Adv. Sci. 3, 1500256.
Dinh, T., Phan, H.P., Kozeki, T., Qamar, A., Fujii, T., Namazu, T., Nguyen, N.T., Dao, D.V., 2016. High thermosensitivity of silicon nanowires induced by amorphization. Mater. Lett. 177, 80–84.
Dinh, T., Phan, H.-P., Nguyen, T.-K., Qamar, A., Woodfield, P., Zhu, Y., Nguyen, N.-T., Dao, D.V., 2017. Solvent-free fabrication of biodegradable hot-film flow sensor for noninvasive respiratory monitoring. J. Phys. D: Appl. Phys. 50, 215401.
Dinh, T., Dau, V., Tran, C.-D., Nguyen, T.-K., Phan, H.-P., Nguyen, N.-T., Dao, D.V., 2019. Polyacrylonitrile-carbon nanotube-polyacrylonitrile: a versatile robust platform for flexible multifunctional electronic devices in medical applications. Macromol. Mater. Eng. 304, 190014.
Falahi, H., Zhang, J., Phan, H.-P., Nguyen, N.-T., 2019. Flexible microfluidics: fundamentals, recent developments, and applications. Micromachines 10, 830.
Hunter, G.W., Okojie, R.S., Neudeck, P.G., Beheim, G.M., Ponchak, G.E., Fralick, G., Wrbanek, J., Chen, L.Y., 2006. High temperature electronics, communications, and supporting technologies for Venus missions. Electr. Eng. 8.
Hwang, S.W., Lee, C.H., Cheng, H., Jeong, J.W., Kang, et al., 2015. Biodegradable elastomers and silicon nanomembranes/nanoribbons for stretchable, transient electronics, and biosensors. Nano Lett. 15, 2801–2808.
Jeon, J., Lee, H.B.R., Bao, Z., 2013. Flexible wireless temperature sensors based on Ni microparticle-filled binary polymer composites. Adv. Mater. 25, 850–855.
Jeong, J., Essafi, M., Lee, C., Haoues, M., Diouani, M.F., Kim, H., Kim, Y., 2018. Ultrasensitive detection of hazardous reactive oxygen species using flexible organic transistors with polyphenol-embedded conjugated polymer sensing layers. J. Hazard. Mater. 355, 17–24.
Kojima, K., Yoshikawa, M., Ohshima, T., Itoh, H., Okada, S., 2000. Characterization of Au Schottky contacts on p-type 3C-SiC grown by low pressure chemical vapor deposition. Mater. Sci. Forum 338, 1239–1242.
Lanni, L., Malm, B.G., Ostling, M., Zetterling, C.M., 2013. 500°C bipolar integrated OR/NOR gate in 4H-SiC. IEEE Electron Dev. Lett. 34, 1091–1093.
Lee, Y.K., Yu, K.J., Song, E., Barati Farimani, A., Vitale, F., et al., 2017. Dissolution of monocrystalline silicon nanomembranes and their use as encapsulation layers and electrical interfaces in water-soluble electronics. ACS Nano 11, 12562–12572.
Li, Q., Chen, L., Gadinski, M.R., Zhang, S., Zhang, G., Li, H.U., Iagodkine, E., Haque, A., Chen, L.Q., Jackson, T.N., Wang, Q., 2015. Flexible high-temperature dielectric materials from polymer nanocomposites. Nature 523, 576–579.
Li, G., Song, E., Huang, G., Guo, Q., Ma, F., Zhou, B., Mei, Y., 2018. High-temperature-triggered thermally degradable electronics based on flexible silicon nanomembranes. Adv. Funct. Mater. 28 1801448.
Liu, Z., Xu, J., Chen, D., Shen, G., 2015. Flexible electronics based on inorganic nanowires. Chem. Soc. Rev. 44, 161–192.
Mandrusiak, G., She, X., Waddell, A.M., Acharya, S., 2018. On the transient thermal characteristics of silicon carbide power electronics modules. IEEE Trans. Power Electron. 33, 9783–9789.

Meador, M.A., 2019. The role of advanced materials and manufacturing in future NASA exploration missions. In: American Chemical Society National Meeting. USA. 20190025280.
Nassar, J.M., Khan, S.M., Velling, S.J., Diaz-Gaxiola, A., Shaikh, S.F., Geraldi, N.R., Torres Sevilla, G.A., Duarte, C.M., Hussain, M.M., 2018. Compliant lightweight non-invasive standalone "Marine Skin" tagging system. NPJ Flex. Electron. 2, 13.
Nathan, A., Ahnood, A., Cole, M.T., Lee, S., Suzuki, Y., et al., 2012. Flexible electronics: the next ubiquitous platform. Proc. IEEE 100, 1486–1517.
Nguyen, T.K., Phan, H.P., Dinh, T., Han, J., Dimitrijev, S., Tanner, P., Foisal, A.R.M., Zhu, Y., Nguyen, N.T., Dao, D.V., 2017. Experimental investigation of piezoresistive effect in p-type 4H-SiC. IEEE Electron Dev. Lett. 38, 955–958.
Nguyen, T.K., Phan, H.P., Dinh, T., Foisal, A.R.M., Nguyen, N.T., Dao, D.V., 2018. High-temperature tolerance of the piezoresistive effect in p-4H-SiC for harsh environment sensing. J. Mater. Chem. C 6, 8613–8617.
Nguyen, T., Dinh, T., Foisal, A.R.M., Phan, H.-P., Nguyen, T.-K., Nguyen, N.-T., Dao, D.V., 2019. Giant piezoresistive effect by optoelectronic coupling in a heterojunction. Nat. Commun. 10, 4139.
Phan, H.-P., Dowling, K.M., Nguyen, T.-K., Chapin, C.A., Dinh, T., Miller, R.A., Han, J., Iacopi, A., Senesky, D.G., Dao, D.V., Nguyen, N.-T., 2018. Characterization of the piezoresistance in highly doped p-type 3C-SiC at cryogenic temperatures. RSC Adv. 8, 29976–29979.
Phan, H.-P., Zhong, Y., Nguyen, T.-K., Park, Y., Dinh, T., et al., 2019a. Long-lived, transferred crystalline silicon carbide nanomembranes for implantable flexible electronics. ACS Nano 13, 11572–11581.
Phan, H.P., Nguyen, T.K., Dinh, T., Qamar, A., Iacopi, A., Lu, J., Dao, D.V., Rais-Zadeh, M., Nguyen, N.T., 2019b. Wireless battery-free SiC sensors operating in harsh environments using resonant inductive coupling. IEEE Electron Dev. Lett. 40, 609–612.
Qamar, A., Dao, D.V., Han, J., Phan, H.P., Younis, A., Tanner, P., Dinh, T., Wang, L., Dimitrijev, S., 2015. Pseudo-Hall effect in single crystal 3C-SiC (111) four-terminal devices. J. Mater. Chem. C 3, 12394–12398.
Rogers, J.A., Someya, T., Huang, Y., 2010. Materials and mechanics for stretchable electronics. Science 327, 1603–1607.
Shaikh, S.F., Mazo-Mantilla, H.F., Qaiser, N., Khan, S.M., Nassar, J.M., Geraldi, N.R., Duarte, C.M., Hussain, M.M., 2019. Noninvasive featherlight wearable compliant "Marine Skin": standalone multisensory system for deep-sea environmental monitoring. Small 15, 1804385.
So, H., Senesky, D.G., 2017. Effect of frost formation on operation of GaN ultraviolet photodetectors at low temperatures. IEEE Sensors J. 17, 4752–4756.
Sun, Y., Rogers, J.A., 2007. Inorganic semiconductors for flexible electronics. Adv. Mater. 19, 1897–1916.
Sun, B., Sun, Y., Wang, C., 2018. Flexible transparent and free-standing SiC nanowires fabric: stretchable UV absorber and fast-response UV-A detector. Small 14, 1703391.
Wang, L., Dimitrijev, S., Han, J., Tanner, P., Iacopi, A., Hold, L., 2011. Demonstration of p-type 3C-SiC grown on 150 mm Si (100) substrates by atomic-layer epitaxy at 1000C. J. Cryst. Growth 329, 67–70.
Yang, T., Chen, S., Li, X., Xu, X., Gao, F., Wang, L., Chen, J., Yang, W., Hou, X., Fang, X., 2019a. High-performance SiC nanobelt photodetectors with long-term stability against 300°C up to 180 days. Adv. Funct. Mater. 29, 1806250.
Yang, J., Feng, J., Li, W., Chen, X., Liu, X., Ruan, J., Qiu, R., Xiong, Y., Tian, S., 2019b. A resource-utilization way of the waste printed circuit boards to prepare silicon carbide nanoparticles and their photocatalytic application. J. Hazard. Mater. 373, 640–648.
Yin, L., Farimani, A.B., Min, K., Vishal, N., Lam, J., Lee, Y.K., Aluru, N.R., Rogers, J.A., 2015. Mechanisms for hydrolysis of silicon nanomembranes as used in bioresorbable electronics. Adv. Mater. 27, 1857–1864.
Yu, K.J., Yan, Z., Han, M., Rogers, J.A., 2017. Inorganic semiconducting materials for flexible and stretchable electronics. NPJ Flex. Electron. 1, 1–14.
Zhan, Y., Mei, Y., Zheng, L., 2014. Materials capability and device performance in flexible electronics for the Internet of Things. J. Mater. Chem. C 2, 1220–1232.
Zhang, Y., Ma, C., Lu, X., Liu, M., 2019. Recent progress on flexible inorganic single-crystalline functional oxide films for advanced electronics. Mater. Horizons 6, 911–930.